Femtolens Imaging of a Quasar Central Engine
Using a Dwarf Star Telescope

Andrew Gould[1]

and

B. Scott Gaudi

Dept of Astronomy, Ohio State University, Columbus, OH 43210

e-mail gould@payne.mps.ohio-state.edu, gaudi@payne.mps.ohio-state.edu

Abstract

We show that it is possible to image the structure of a distant quasar on scales of $\sim 1\,\mathrm{AU}$ by constructing a telescope which uses a nearby dwarf star as its "primary lens" together with a satellite-borne "secondary". The image produced by the primary is magnified by $\sim 10^5$ in one direction but is contracted by 0.5 in the other, and therefore contains highly degenerate one-dimensional information about the two-dimensional source. We discuss various methods for extracting information about the second dimension including "femtolens interferometry" where one measures the interference between different parts of the one-dimensional image with each other. Assuming that the satellite could be dispatched to a position along a star-quasar line of sight at a distance r from the Sun, the nearest available dwarf-star primary is likely to be at $\sim 15\,\mathrm{pc}\,(r/40\,\mathrm{AU})^{-2}$. The secondary should consist of a one-dimensional array of mirrors extending $\sim 700\,\mathrm{m}$ to achieve 1 AU resolution, or $\sim 100\,\mathrm{m}$ to achieve 4 AU resolution.

Subject Headings: gravitational lensing – instrumentation: interferometers – quasars: general

---

1 Alfred P. Sloan Foundation Fellow

1. Introduction

Gravitational microlensing by Galactic stars (and possibly other objects) has been detected in more than 100 events seen toward the Galactic bulge by MACHO (Alcock et al. 1996), OGLE (Udalski et al. 1994), and DUO (Alard 1996). Generally, these stellar lenses are believed to be several kpc from the Sun, either in the Galactic bulge or in distant regions of the Galactic disk.

There have been several suggestions to make use of more nearby stars as lenses. Nearby stars have high proper motions and relatively large Einstein rings. One could predict when they would lens more distant stars, measure the Einstein ring and so determine the mass of the lensing star (Paczyński 1995). Even if the projected separation between the nearby and distant stars is many Einstein radii, the former will still deflect the light of the latter. This effect could be measured using interferometry and would again yield a mass measurement (Miralda-Escudé 1996). Extremely nearby objects could conceivably be detected by diffractive lensing flashes (Labeyrie 1994).

Here we propose a more ambitious use of a nearby star as the primary lens of a telescope whose purpose would be to resolve the central engine of a quasar. Since quasars lie at an angular-diameter distance $D_Q \sim 10^9$ pc, and since their central engines are believed to have dimensions $\mathcal{O}(\text{AU})$, such a telescope would require an effective resolution of 10^{-9} arcsec, roughly the equivalent of an optical interferometer with an Earth-Moon baseline. In general, previous suggestions for the use of nearby stars have assumed that one must wait for the lens and source to line up with the Earth. The probability for the required alignment with a quasar is negligibly small. However, if Mohammed will not go to the mountain ...

2. Characteristics of the Primary Lens

To construct the telescope, there must be a dwarf star aligned with a quasar as seen from *somewhere* in the solar system. For definiteness, we define "somewhere" as being within a distance $r = 40\,\mathrm{AU}$ of the Sun. For a star at distance D, the quasar must then lie within an angle r/D of the star (as seen from the Sun). The probability of such an occurrence is $\pi(r/D)^2 N_Q$, where $N_Q = 200\,\mathrm{deg}^{-2}$ is the angular density of quasars brighter than $B = 22$ (Hartwick & Schade 1990). The expected number of such alignments by dwarfs within a distance D_{lim} of the Sun is then

$$\int_0^{D_{\mathrm{lim}}} dD\, 4\pi D^2 \pi \left(\frac{r}{D}\right)^2 n N_Q = 4\pi^2 r^2\, D_{\mathrm{lim}} n N_Q \sim \frac{D_{\mathrm{lim}}}{15\,\mathrm{pc}}, \tag{2.1}$$

where we have assumed a local density of dwarfs of $n = 0.07\,\mathrm{pc}^{-3}$ (Gould, Bahcall, & Flynn 1996 and references therein). Even if no such dwarfs are present at a given time, a statistically independent sample will be available after a duration $r/v \sim 5\,\mathrm{years}$, where we have adopted $v \sim 40\,\mathrm{km\,s}^{-1}$ as the typical transverse speed of disk stars.

We now assume that such a star has been identified at a distance $D \sim 15\,\mathrm{pc}$ and mass $M \sim 0.4 M_\odot$. We further assume that a satellite has been equipped with the remaining optics that are required for construction of the telescope and that it has been dispatched to a position along the dwarf-quasar line of sight. Note that the satellite must not only be in the correct location, but must also be moving with the same transverse velocity as the dwarf star ($\sim 40\,\mathrm{km\,s}^{-1}$) so that the alignment with the quasar is maintained.

The first job of the satellite will be to measure the optical properties of the primary lens. The distance to the lens will be very accurately known from parallax measurements. Hence the mass can be determined from the angular size of the Einstein ring $\theta_e = (4GM/c^2 D)^{1/2}$. Since the quasar is at a cosmological distance, its light will be affected by a gravitational shear due to mass distributed near the

line of sight. This shear combines with the point-mass lens (the dwarf star) to produce a Chang-Refsdal lens (Chang & Refsdal 1979). Such lenses are completely described by the angular size of the Einstein ring, θ_e, the magnitude of the shear, γ, and the orientation of the shear. The magnitude of the shear will not be known *a priori*, but based on initial measurements or possibly upper limits (Villumsen 1996), we assume $\gamma \sim 1\%$. For $\gamma \ll 1$ it is easy to show (using e.g. the formalism of Gould & Loeb 1992) that the lens has a diamond-shaped caustic with an angular distance between opposite cusps $\sim 4\gamma\theta_e$. Hence one could measure γ by moving the spacecraft so as first to align the quasar with one of the cusps and then measuring the distance to the opposite cusp. For our adopted parameters, $\theta_e \sim 10\,\mathrm{mas}$ and the distance between cusps is $4\gamma D\theta_e = 6 \times 10^{-3}\,\mathrm{AU}$. The orientation of the caustic is along the line connecting the star and the quasar image when the quasar is at the cusp.

3. Characteristics of the Satellite

To resolve the central engine of the quasar, the satellite must situate itself so that the center of the quasar lies inside the caustic and very near the cusp. Let (ξ, η) be the coordinates of source plane in units of the Einstein ring. One may equally well think of these as coordinates of the observer plane with corresponding physical distances $(D\theta_e\xi, D\theta_e\eta)$. Let $\Delta\xi$ be the distance along the ξ axis from the cusp at $\xi \sim 2\gamma$. One finds that the caustic in the neighborhood of the cusp is reasonably well described by $\eta^2 = (\Delta\xi)^3/4\gamma$. Thus, a source with angular radius $\rho\theta_e$ can come as close as $\Delta\xi \sim (4\gamma\rho^2)^{1/3}$ while still remaining inside the caustic. For sources lying on the ξ axis, the magnification tensor of the brightest image is diagonal, with diagonal components $(\Delta\xi^{-1}, 0.5)$. Hence, a source of size $\rho\theta_e \sim AU/D_Q \sim 10^{-9}$ arcsec is stretched by a factor $\sim 1.4 \times 10^5$ and would therefore subtend an angle $\theta_r \sim 140\mu\mathrm{as}$.

If the quasar were observed in optical light ($\lambda \sim 0.5\,\mu\mathrm{m}$), an effective aperture $\lambda/\theta_r \sim 700\,\mathrm{m}$ would be required to resolve this angle. The required aperture

is therefore smaller than the full width caustic, $2D\rho\theta_e \sim 5\,\mathrm{km}$, implying that the entire effective aperture would fit well inside the caustic projected onto the observer plane. This is an essential ingredient for making the observations. It is impractical and unnecessary to fill the entire aperture with mirrors. In fact, only one dimension must be well sampled because the quasar image is essentially one dimensional: it is highly stretched in one direction and slightly contracted in the other. Even the image of the region ~ 2000 AU around the quasar would have a lateral extent of only $\sim 1\,\mu\mathrm{as}$, far too small to be resolved. Of course, it will be necessary to remove the light from the lensing star which will be separated from the quasar image by $\theta_e \sim 10^4\,\mu\mathrm{as}$ and will typically subtend $\sim 300\,\mu\mathrm{as}$. Most of this light could be directed to a position well off the image center simply by tilting the axis of the array $\sim 20°$ relative to the critical curve. There would still be some contamination from the high-order fringes but much of this could be removed provided that the width of the mirror array were a few tens of meters.

To remain in the caustic over time, the satellite must counter the acceleration due to the Sun at a distance of 40 AU, which is $\sim 4 \times 10^{-4}\,\mathrm{cm\,s^{-2}}$. After 10 hours of such acceleration, the satellite will have drifted $\sim 3\,\mathrm{km}$ and will require a boost of $\sim 20\,\mathrm{cm\,s^{-1}}$ to get back on track. The energy required for these repeated boosts is negligible compared to that needed to achieve the initial velocity. However, stabilization of the mirror system following the boosts might prove to be a significant engineering challenge.

4. Information in One and Two Dimensions

The source regions inside the caustic are mapped into four images. For a point source near the cusp, three of these images are highly magnified and lie close to the critical curve on the same side of lensing star as the quasar. The fourth image lies on the opposite side of the star. It is not highly magnified and will not be considered further. For $\gamma \ll 1$, the critical curve deviates only slightly from the Einstein ring of an isolated lens. The central image is the brightest and lies just
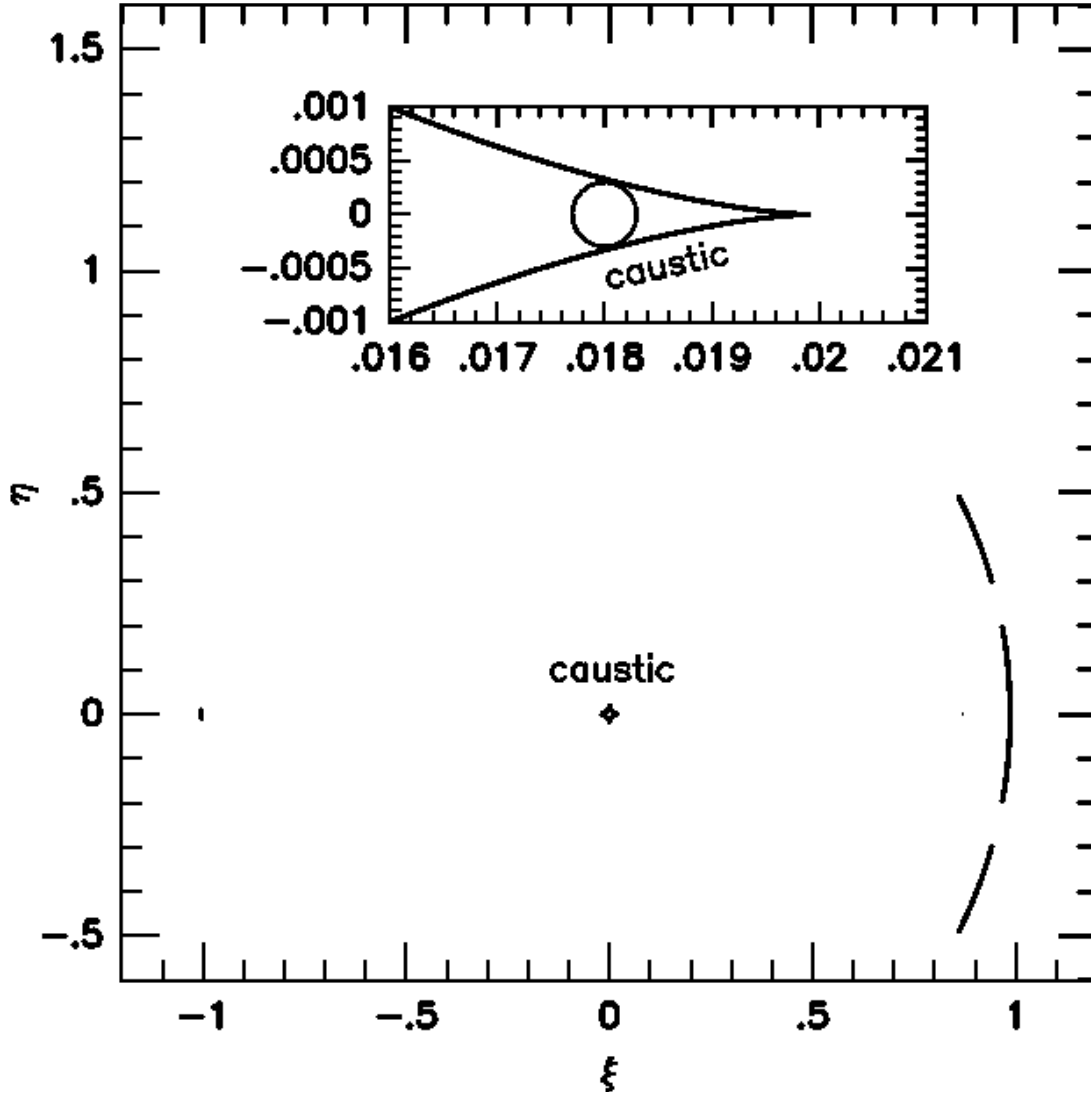
Figure 1. Primary lens geometry. Source lies entirely inside the caustic and near one cusp. It is therefore lensed into four images, three of which are highly magnified and lie very close to the critical curve to the right. Note that they are essentially one-dimensional. The fourth image (to the left) is not highly magnified. The inset shows a close up of the source within the caustic. For this illustrative example, the source is stretched only by a factor $\sim 10^2$ compared to factors $\sim 10^5$ generally considered in this paper.

outside the critical curve. The other two images lie just inside the critical curve and the sum of their magnifications is nearly equal to that of the central image. Each image with magnification A is stretched by a factor $2A$ along the critical curve and compressed by a factor 0.5 perpendicular to it. See Figure 1.
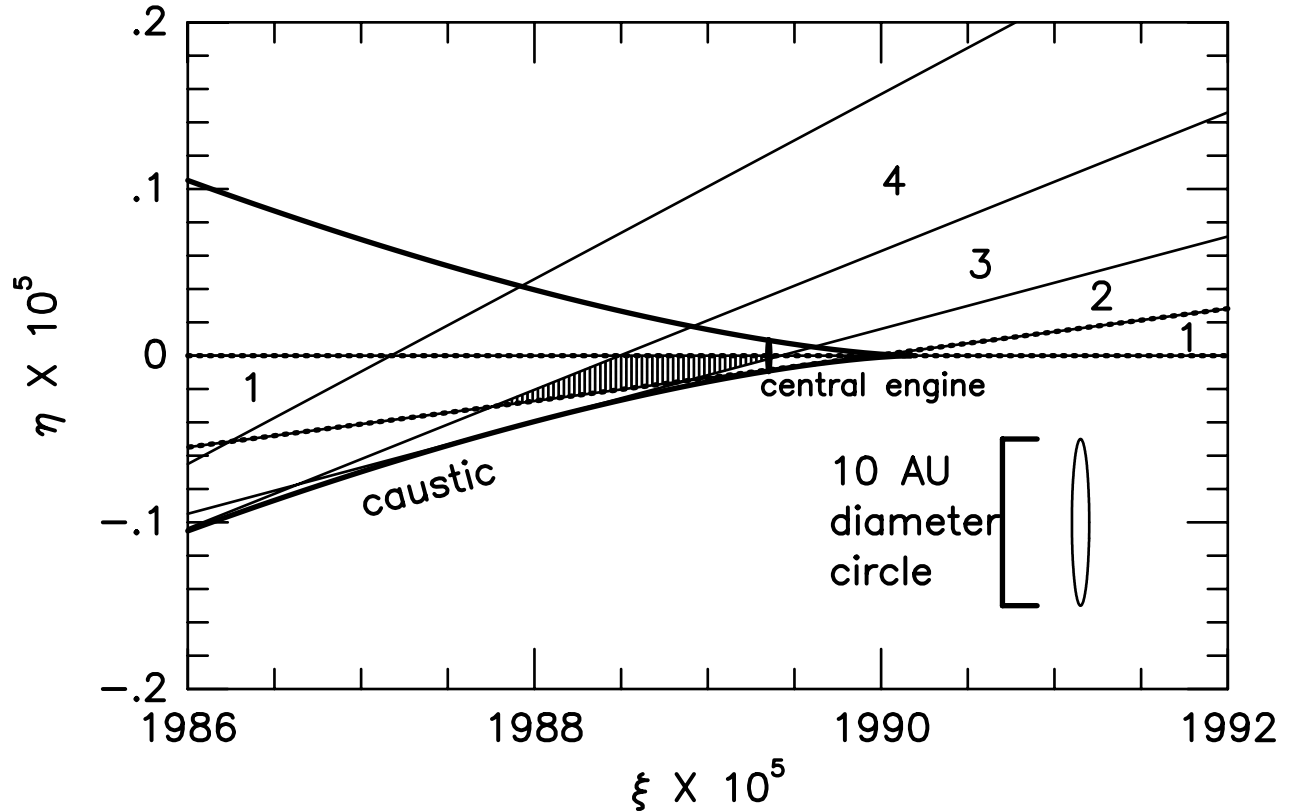
Figure 2. Bands of image degeneracy. The bold curve is the caustic within which there are three images. All three images lie in an almost one-dimensional structure close to the critical curve. All the points in the source between two adjacent solid lines are mapped into the same resolution element ($\sim 140\,\mu$as) along the critical-curve image. The bands are labeled 1, 2, 3, and 4. Band 1 is marked with a dotted line. The 10 AU circle at the lower right indicates the scale and distortion of the figure which, for reasons of clarity, is stretched by a factor 10 in the vertical direction. A smaller circle of radius 1 AU is marked "central engine". Note that it is resolved into two resolution elements.

In principle, since each point of the source is mapped into three unique points of the image, one can reconstruct the source from the image. In fact, all three images are compressed into a one dimensional curve whose angular width is approximately equal to that of the unlensed source. As mentioned above, this means that a region of 2000 AU is compressed into a curve of width $\sim 1\,\mu$as, far smaller than the resolution element. Thus, in practice each resolution element ("point") along the critical curve represents the sum of the contributions from an entire curve within the source. These "degeneracy curves" are actually almost perfectly straight lines

and are tangent to the caustic at exactly one point. Since the resolution element has finite width, the "degeneracy curves" are in fact "degeneracy bands" whose width shrinks as it approaches the tangent point and then expands again. See Figure 2.

The nature of this degeneracy can be understood by considering a quasar with a central engine of radius $\sim 1\,\mathrm{AU}$, but which is emitting significant amounts of light over a radius $\sim 200\,\mathrm{AU}$. As discussed above, the central AU is imaged into a rectangular arc about $100\,\mu\mathrm{as}\times 10^{-3}\,\mu\mathrm{as}$. Other regions of the quasar of intrinsic width 1 AU will be mapped into the same $100\,\mu\mathrm{as}$, also with width $10^{-3}\,\mu\mathrm{as}$. The relative contributions of these different regions to the observed light will scale according to their surface brightnesses. Thus, if the entire quasar had the same surface brightness, the central engine would contribute only $\sim 1/200$ of the light to this resolution element of the image. If surface brightness fell inversely with radius, it would contribute a fraction $1/\ln(200) \sim 20\%$.

There are several methods for breaking this degeneracy. The first is to make use of the three images. A most spectacular example of this approach is the recent resolution of an apparent ring galaxy using multiple images produced by a cluster lens (Colley, Tyson, & Turner 1996). If there is a significant excess brightness of the middle image due to a hot central engine, this excess will also be apparent at the locations of the two other images.

There is also a second more powerful method. As the satellite drifts over the central regions of the quasar, the point in the source that is nearest the cusp and which is therefore maximally magnified varies. The positions within the caustic structure of all other points in the source also vary, but the change in their magnifications with position is much smaller. Thus, one could map out the brightness of the inner regions. The second and third images would serve as a check on these measurements. Of course, this approach requires that the brightness profile of the quasar remain relatively constant during the series of observations.

5. Femtolens Interferometry

Still another method is to look for interference effects between images. A number of authors have discussed the possibility of observing "femtolensing", interference between the *integrated light* of two or more images (Mandzhos 1981; Schneider & Schmidt-Burgk 1985; Deguchi & Watson 1986; Peterson & Falk 1991; Gould 1992; Ulmer & Goodman 1995). Here we analyze the possible role of such interference in the *two-dimensional reconstruction* of the source. The principle is relatively simple. As shown in Figure 2, each resolution element of the one-dimensional image along the critical curve corresponds to a band of variable width in the source plane. Consider the two bands labeled "1" and "3". Suppose that the light falling on the two corresponding resolution elements is brought together and then dispersed in a spectrograph. Most of the light in each resolution element comes from regions of the source that are unrelated to the regions that generate the light entering the other element. This light does not suffer any effects of interference. However, the light coming from the small shaded region where the two sets of curves cross arrives at the two images "1" and "3" at times t_1 and t_3 and therefore suffers interference according to a time lag $\Delta t_{1,3} = t_1 - t_3$. Hence, there will be an oscillation in the spectrum with frequency spacing $\Delta f_{1,3} = (\Delta t_{1,3})^{-1}$. Such an oscillation is observable provided the spectrograph has a resolving power $R \gtrsim ct_{1,3}/\lambda$ and, of course, provided it has sufficient amplitude to be seen above the noise of the remaining photons that do not participate in the fluctuation.

It is actually possible to substantially further improve the resolution. In the previous treatment, we imagined that the time delay between the "1" and "3" images is constant over the entire overlap region shown in Figure 2. If this were so, the interference term would scale with frequency f as $\sin^2(2\pi f/f_{1,3})$. In fact, the time delay is a function of position within the patch, ranging from $\Delta t_{1,3,\mathrm{min}} = 2\lambda/c$ to $\Delta t_{1,3,\mathrm{max}} = 33\lambda/c$, where $\lambda = 0.5\mu$m. In Figure 3, we show a blow-up of the overlap region with 10 contours of constant time delay between the images in resolution elements "1" and "3". By taking the Fourier transform of
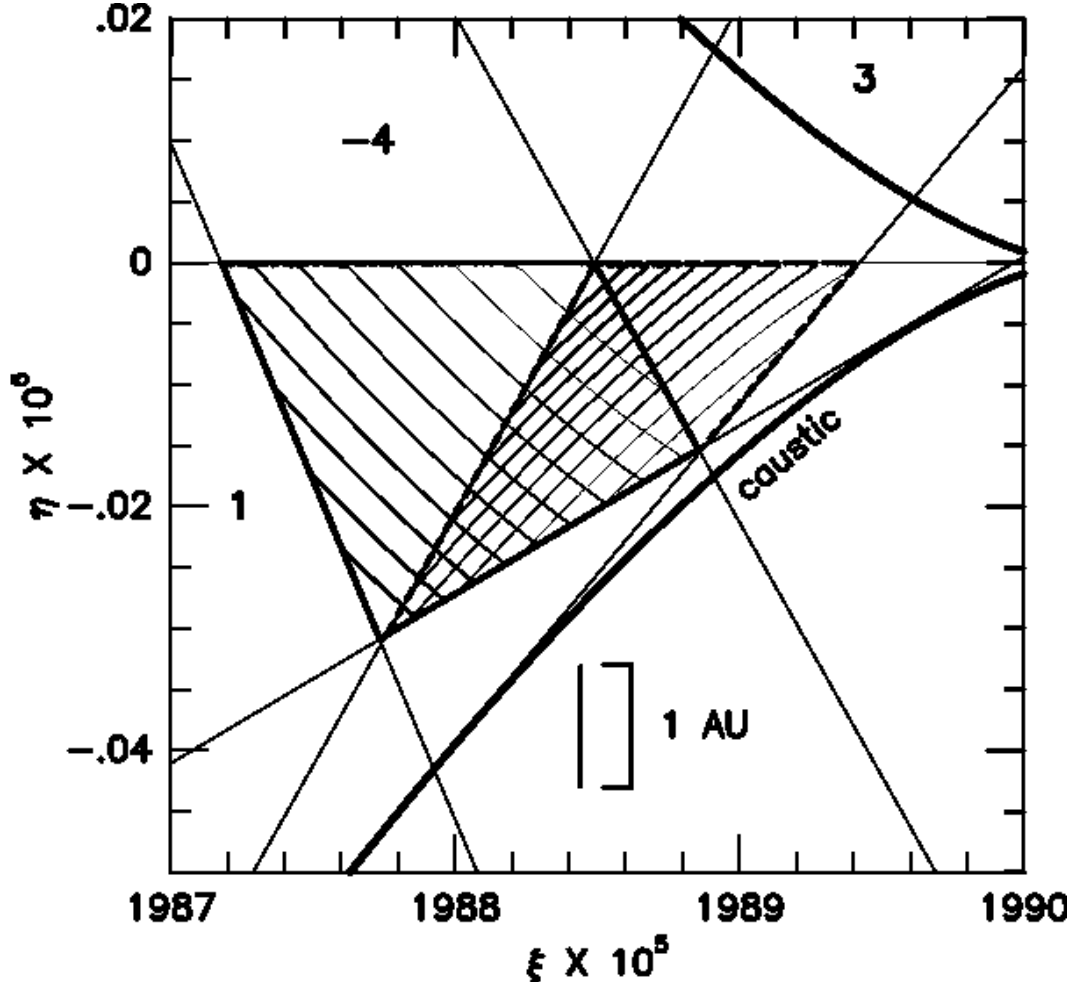
Figure 3. Overlap between source resolution elements "1" and "3" from Fig. 2 (*bold dashed quadrangle*) subdivided into ten zones of equal time delay between the two images (*solid up-right diagonal curves*). The total light in each zone can be determined by Fourier analysis of the interference resolution elments "1" and "3". The overlap between source resolution elements "1" and "–4" (*bold quadrangle*) is also divided into ten zones of equal delay between images "1" and "–4" (*solid up-left diagonal curves*). A similar (approximately horizontal) set of contours could also be drawn for the delay structure between images "3" and "–4" but is not shown to avoid clutter. These measurements could produce resolution that is substantially finer than the naive result indicated in Fig. 2.

the interference pattern produced by combining these two resolution elements, one could determine how much of the source light lay between pairs of consecutive

10

contours. Of course, the choice of 10 contours was arbitrary. One could in principle resolve the region into up to the diffraction limit of ~ 30 bands at which point the adjacent time delays would differ by only $\sim \lambda/c$. There is also a third image. For the left hand side of the overlap region this image lies in resolution element "–4", and for the right hand side it lies in element "–3". We focus on the first. One can now repeat the same procedure for the interference patterns generated by the time delays $\Delta t_{1,-4}$ (see Fig. 3) and $\Delta t_{3,-4}$, thereby further constraining the structure within the patch. Note that while the one-dimensional resolution is limited only by the diffraction limit, the true two-dimensional resolution is not as small as the grid shown in Figure 3, since there are 100 such patches in an overlap region (assuming 10 contours in each direction), but only 30 pieces of information from the three sets of contours. Nevertheless, it would be possible to track isolated blobs having the size of one of the patches shown in Figure 3, and thus in this restricted sense the figure is indicative of the effective resolution.

6. Photons

It would be premature to attempt a detailed estimate of the signal-to-noise ratios in this proposed experiment. However, it is legitimate to ask whether these ratios are closer to 10^2 or 10^{-2}. Suppose that the quasar magnitude is $V = 22$ and that 10% of the quasar light comes out in the *annulus* containing the shaded overlap region in Figure 2. The fraction of the total light produced by the overlap region is then $\sim 2 \times 10^{-4}$. The typical magnifications in this region are $\sim 3 \times 10^4$, i.e, each image has a (magnified) apparent magnitude $V \sim 20$. If we suppose that the total area of the telescope were $20 \, \mathrm{m}^2$, then the number of photons collected from this region during a 1 hour exposure would be $\mathcal{O}(10^6)$. If there were ~ 10 times more photons from non-overlap regions, the signal-to-noise ratio would be ~ 300, an ample number to measure not only the total flux from the region, but substantial substructure as well. Thus it would be possible to follow the detailed evolution of the quasar on time scales comparable to the light crossing time.

REFERENCES

1. Alard, C. 1996, in Proc. IAU Symp. 173 (Eds. C. S. Kochanek, J. N. Hewitt), in press (Kluwer Academic Publishers)

2. Alcock, C., et al. 1996, ApJ, submitted

3. Chang, K., & Refsdal, S. 1979, Nature, 282, 561

4. Colley, W. N., Tyson, J. A., & Turner, E. L. 1996, ApJ, 461, L83

5. Deguchi, S., & Watson, W. D. 1986, ApJ, 307, 30

6. Gould, A. 1992, ApJ, 386, L5

7. Gould, A., Bahcall, J. N., & Flynn 1996, ApJ, 465, 000

8. Gould, A., & Loeb, A. 1992, ApJ, 396, 104

9. Hartwick, R. D. A. & Schade, D. 1990, AARA, 28, 437

10. Labeyrie, A. 1994, A&A, 284, 689

11. Mandzhos, A. V. 1981, Soviet Astron. Lett., 7, 213

12. Miralda-Escudé, J., 1996, ApJL, submitted

13. Paczyński, B. 1995, Acta Astr., 45, 345

14. Peterson, J. B., & Falk, T. 1991, ApJ, 374, L5

15. Schneider, P., & Schmidt-Burgk, J. 1985, A&A, 148, 369

16. Udalski, A., et al. 1994, Acta Astronomica 44, 165

17. Ulmer, A., & Goodman, J. 1995, ApJ, 442, 67

18. Villumsen, J. V. 1996, MNRAS, submitted